NOTES

Limnol. Oceanogr., 46(7), 2001, 1774–1780

Atlantic climate governs oceanographic and ecological variability in the Barents Sea

Abstract—In the arcto-boreal Barents Sea, temperature variability is an important source for the pronounced year-to-year fluctuations in fish recruitment. Sea temperature is closely linked to the volume flux of the relatively warm Atlantic water masses flowing in from southwest, as well as to regional heat exchange with the atmosphere. We examine the relations between Barents Sea temperature, inflow, and North Atlantic scale climate variability. For the last three decades, large-scale climate forcing statistically has accounted for 75% of the variability in the barotrophic inflow, whereas the North Atlantic Oscillation and sea temperature combined statistically explain 55% of the variability in cod recruitment. Our results suggest a chain-of-events relationship between large-scale atmospheric variability, Barents Sea oceanography and the ecology of this highly productive region.

The northeast Atlantic region of the Barents Sea (Fig. 1) is a highly productive region, being the home to the world's largest stock of cod (*Gadus morhua*) and nursery ground for the largest herring (*Clupea harengus*) stock. However, recruitment and growth of these commercially important fish stocks varies extensively. In this article, we document how North Atlantic climate fluctuations during the past three decades has affected the Barents Sea environment and, ultimately, the population dynamics of fish in the region.

The Barents Sea is an open arcto-boreal shelf sea. Year-to-year variability in sea temperatures is profoundly influenced by the relatively warm Atlantic water masses flowing in from southwest (Loeng 1991) as well as regional heat exchange with the atmosphere (Ådlandsvik and Loeng 1991; Loeng et al. 1992). The interannual variability is, to a large extent, determined by conditions during winter, the season when the differences in temperature both between inflowing and local water masses and between the local atmosphere and the sea surface are at their highest.

The Arcto-Norwegian cod spawn in March–May in patchy areas off mid- and northern Norway. Eggs and larvae follow the currents toward the north and east and are spread all over the southern Barents sea and southwest of Spitsbergen, 600–1200 km from their spawning ground, when they settle toward the bottom at age ~5 mo. At this stage, year-class strength is already mainly determined (Sundby et al. 1989).

The impact of interannual and decadal shifts in regional climate, sea temperature in particular, on recruitment of fish in the Barents Sea has been well documented (see Sætersdal and Loeng 1987 and Ottersen and Sundby 1995 for references). A positive impact on fish of above-normal sea temperatures is reasonable, given that ''warm'' years are good years productionwise in the Barents Sea for three principal reasons: (1) a larger ice-free area allows for higher primary productivity; (2) warm years imply large influxes of zooplankton from the south into the Barents Sea, and (3) higher temperatures lead to higher biological activity at all trophic levels (Sakshaug 1997).

The North Atlantic Oscillation (NAO), an alternation in the sea level air pressure difference between the Azores high and Icelandic low (Fig. 1), is an important source of seasonal to decadal-scale climatic variability in the North Atlantic sector (Hurrell 1995). It quantifies atmospheric large-scale fluctuations between the subtropical and subpolar regions of the North Atlantic and is the dominant mode of atmospheric behaviour in the sector throughout the year, although it is most pronounced during winter.

Earlier authors have related NAO variability to a number of climatic factors throughout the North Atlantic region including speed and direction of the prevailing westerly winds and high atmospheric and sea temperatures in Western Europe (Fromentin and Planque 1996; Dickson 1997). Recently, the important role of the NAO in determining oceanographic and ecological variability in the Baltic was described by Haenninen et al. (1999).

The Gulf Stream separates from the coast of North America near Cape Hatteras (33°N, 75°W) before extending eastward across the North Atlantic. In addition to variability involving large meanders, frequently accompanied by eddies, the position of the Gulf Stream undergoes long-term changes of latitude. The latitudinal position of the north wall of the Gulf Stream has been used as an indicator of climatic fluctuations over the North Atlantic (Taylor 1995).

The Polar/Eurasian pattern (PolEur) consists of one main anomaly center of sea-level air pressure over the polar region and separate centers of opposite sign to the polar anomaly over central Europe and northeastern China. The pattern reflects major changes in the strength of the circumpolar circulation and reveals the accompanying systematic changes that occur in the midlatitude circulation over large portions of Europe and Asia. The pattern appears only in the winter and is the most prominent mode of low-frequency variability in the Northern Hemisphere during December and February.

Data—Monthly values of atmospherically driven water volume flux through the Fugløya-Bear Island section (Figs. 1, 2) have been estimated through a numerical model for the period 1970–1998 (Ådlandsvik and Loeng 1991; Loeng et al. 1992; B. Ådlandsvik pers. comm.). The model is a three-dimensional level model with linear shallow-water equations and vertical eddy viscosity and is discretized by finite dif-

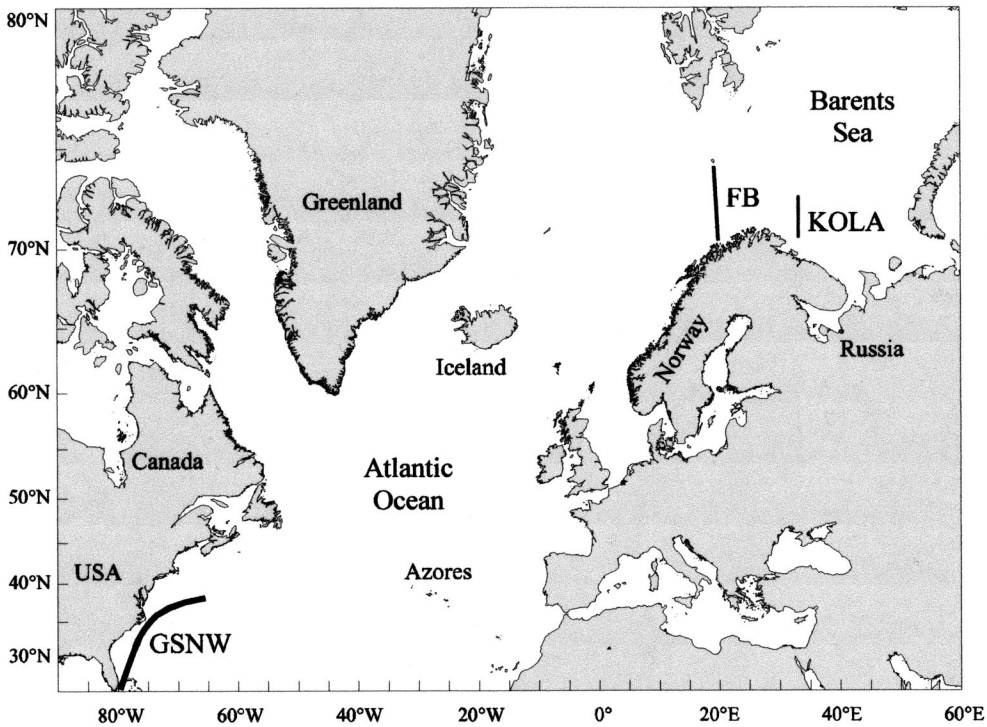

Fig. 1. The North Atlantic and Barents Sea with locations of the studied time series indicated. Atmospherically driven inflow has been modeled for the Fugløya-Bear Island section (FB) and sea temperature observed along the Kola transect (KOLA). The position of the GSNW is indicated by the thick line. The locations of the centers of the dynamics of the NAO, the Icelandic low, and the Azores high are shown.

ferences by use of the Arakawa-C grid. The implementation for the Barents Sea has a horizontal grid resolution of ~20 km (Ådlandsvik and Loeng 1991). The atmospheric forcing is taken from the Norwegian Meteorological Institute's Hindcast Archive, which contains 6-hourly values on a 75-km grid covering all seas around Norway. We use winter (January–April) averages. Density-driven (baroclinic) currents are not included in the model; hence, the flux (F_{FB}) reflects only the variability in atmospheric forcing (barotropic component). The mean F_{FB} for the period 1970–1998 is small compared with available estimates of total transport (Blindheim 1989; Loeng et al. 1997). However, a substantial part of the *variability* in total inflow seems to be caught in the purely barotropic F_{FB} (Fig. 2 may be compared with values from the references above).

The sea temperature series from the Kola meridian transect (33°30′E, 70°30′N–72°30′N), which intersects the Murman Current in the south central Barents Sea (Figs. 1, 2), is considered a good indicator of thermal conditions for the entire Barents Sea region. The series dates back to the turn of the previous century and had by 1996 been taken more than 900 times, since the 1960s about monthly (Tereshchenko 1996). Monthly values have been calculated by averaging temporally, along the transect and vertically from 0 to 200 m water depth. The historical data have been taken from Bochkov (1982) and Tereshchenko (1996), whereas the most recent values have been provided by PINRO, Murmansk. As for F_{FB}, we use January–April values to represent winter, April historically being the coldest month in the Kola section temperature (T_{Kola}) time series.

NAO indices (Figs. 1, 2), slightly modified from the winter (December–March) index of Hurrell (1995), were obtained from the World Wide Web page of Jim Hurrell of NCAR's Climate and Global Dynamics Division (http://www.cgd.ucar.edu/~jhurrell/nao.html). PolEur (Fig. 2) is only a dominating mode for December–February, so means across these months were calculated from monthly values found at http://www.cpc.noaa.gov/data/teledoc/poleur.html. An index of the north wall of the Gulf Stream (GSNW; Fig. 1), represented by the first principal component derived from measurements of the latitude of the Gulf Stream off the coast of the United States at six different longitudes, is available from 1966 and onward (Taylor 1995). Monthly values were found at the Plymouth Marine Laboratory's World Wide Web page (http://www.pml.ac.uk/gulfstream/inetdat.htm). We used winter means spanning December through April to smooth high month-to-month variability due to Gulf Stream meandering.

Year-class strength of Arcto-Norwegian cod was estimated by the number of recruits to the stock at age 3, VPA_3. The values were taken from the 2000 ICES stock assessment, with use of VPA (virtual population analysis) based on commercial catch statistics (B. Bogstad, Institute of Marine Research, Norway, pers. comm.). We use natural log–transformed values of VPA_3 according to the method of, e.g., Thompson and Page (1989). Because year-class strength for

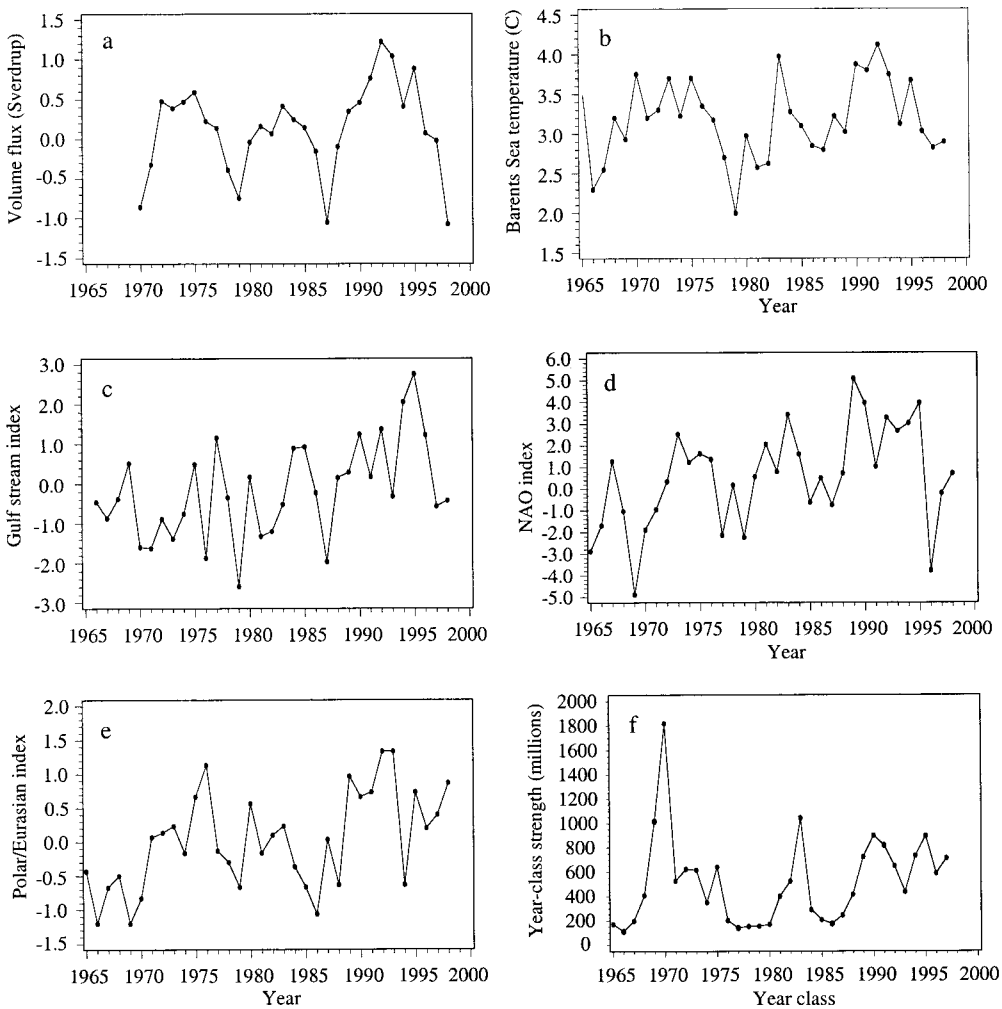

Fig. 2. Time series of winter means of (a) atmospherically driven volume flux through the Fugløya-Bear Island section (F_{FB}), (b) sea temperature (0–200 m depth) observed along the Kola transect (T_{Kola}), (c) the position of the GSNW, (d) the NAO, and (e) PolEur. (f) Year-class strength of Arcto-Norwegian cod estimated as abundance (in millions) at age 3 (VPA_3) . All series are shown from 1965 or when the series started until 1998, *except* VPA_3, until the 1997 year class.

this stock is mainly determined during the first 6 mo of life (Sundby et al. 1989), VPA_3 is compared with the climatic conditions the winter the year class was spawned.

Statistical methods and considerations—Because most of our series were significantly nonstationary according to the test of the unit-root hypothesis (Dickey and Fuller 1979), linear temporal trends were removed by regressing the series (including weighted means) against time (year) and all results derived by analysis of the residuals. Any links found should thus not reflect similarity in trends but indicate close covariability on interannual or decadal scales.

Autoregressive models of order 1, 2, or 3 were evaluated. Maximum-likelihood estimation was used. Terms beyond the first order did not enhance the models performance and were left out in all further calculations. To examine delayed effects, cross-correlations between the various time series were examined for lags 1–5 yr. Three-year weighted means of T_{Kola}, F_{FB}, and the NAO were calculated to take into consideration possible accumulative effects of a prolonged climate state/phase. The current year was weighted 0.5 and each of the two preceding 0.25 (these series are indexed av3).

The period analyzed was restricted to 1972–1998 for models of T_{Kola} to allow performance comparison to include models with 1- and/or 2-yr lagged values or 3-yr weighted means of F_{FB}, this time series beginning in 1970. Because of the above restriction and 1997 being the last year-class with data available at age 3, we were limited to modeling VPA_3 for 1972–1997 (the number of fish spawned in 1997 is estimated by the number of 3-yr-olds in 2000). Otherwise, the period 1970–1998 was considered.

The appropriateness of the models was evaluated by the Akaike Information criterion (AIC) and Schwartz's Bayesian criterion (SBC). For both AIC and SBC lower values indicate the better fit for series of the same length (Priestley 1988). It must be emphasized that AIC or SBC values only can be compared between models for the same phenomena and data set (i.e., F_{FB}, T_{Kola}, or VPA_3).

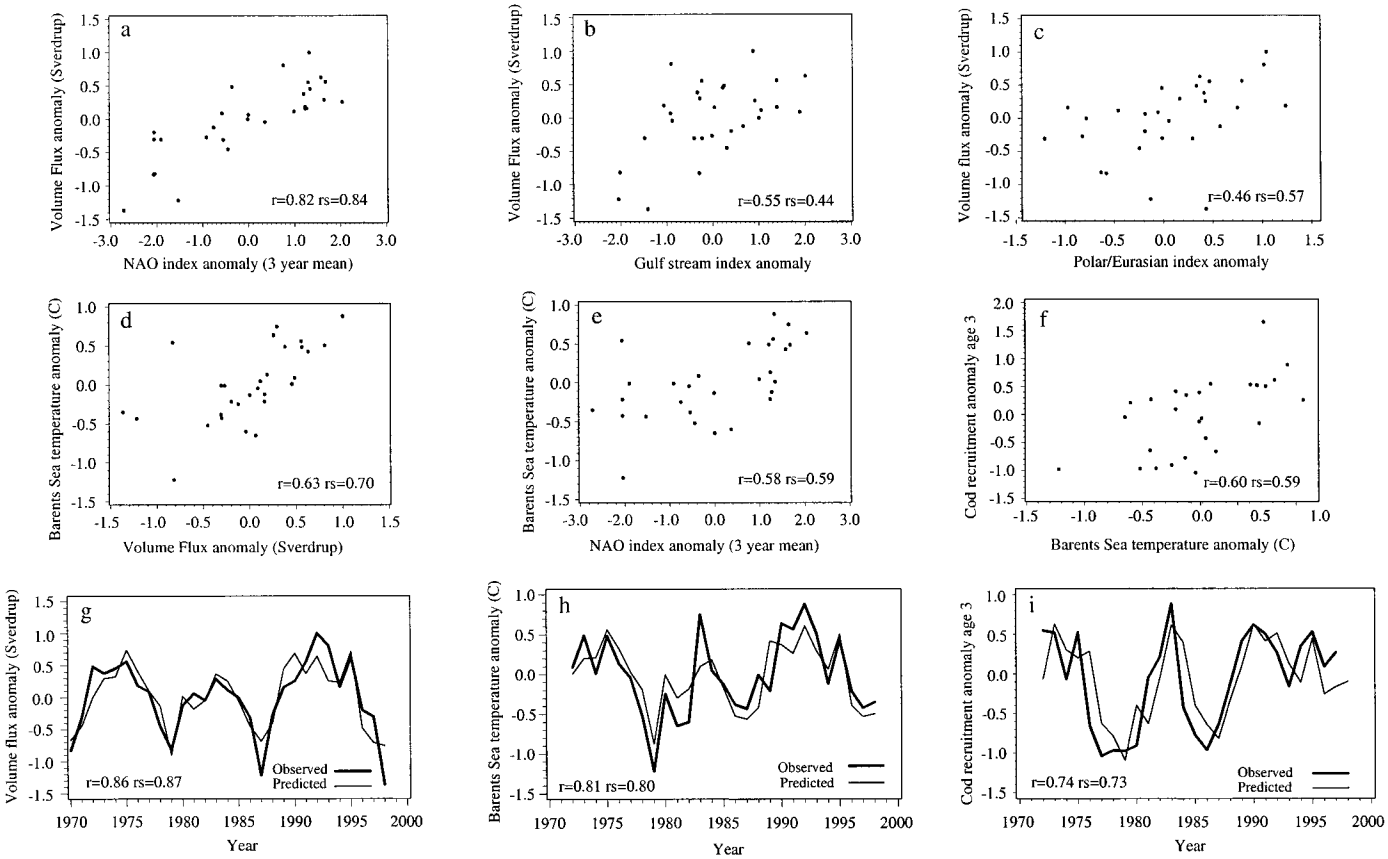

Fig. 3. Correspondence among observed time series and between observed and modelled series (linear trends were first removed by regression against time so that residuals remain; cod recruitment is, in addition, log transformed). Scatter plots compare (a) a mean of the NAO winter index where the current year is weighted 0.5, each of the two previous 0.25 (NAO_{av3}) with atmospherically driven winter inflow through F_{FB}, (b) winter position of the GSNW with F_{FB}, (c) PolEur with F_{FB}, (d) F_{FB} with Kola section 0–200 m depth winter temperatures (T_{Kola}), (e) NAO_{av3} with $T_{Kola,}$ and (f) T_{Kola} with year-class strength of Arcto-Norwegian cod estimated at age 3 (VPA_3) . Observations and predictions from the overall best model are shown for (g) F_{FB}, (h) T_{Kola}, and (i) VPA_3. Pearson product moment (r) and Spearman rank (rs) correlations are given.

Spearman rank correlation was used in addition to Pearson product-moment correlation to allow for nonnormality. In calculating significance levels for correlations, the effective number of independent observations, adjusted for order 1 and 2 autocorrelations (n_e), was estimated by the formula of Quenouille (1952): $n_e = n/(1 + 2r_{a1}r_{b1} + 2r_{a2}r_{b2})$, where n is the number of data points in the two series, r_{a1} and r_{b1} are the lag-one autocorrelations, and r_{a2} and r_{b2} the lag-two autocorrelations.

Results—The time series of F_{FB} and T_{Kola} showed similarities in their fluctuations with the NAO, GSNW, and PolEur pattern (Fig. 2; *see Fig. 1* for locations). All series displayed an increasing trend throughout the period. Furthermore, there were local maxima around 1975, the early to mid-1980s, and again in the early 1990s, after which the values decreased in subsequent years.

Figure 2 does not indicate any strong lagged relations, but a closer enquiry was deemed necessary. Cross correlations between the different climate series confirmed that the highest correlations in most cases were unlagged. It should be noted that the correlation between GSNW and NAO was higher when the former lags the latter with 2 yr than is the direct relationship. Although our cross correlations did not indicate that preceding years values of F_{FB} influence T_{Kola}, earlier results (Ottersen et al. 2000) suggested that such terms might enhance model performance. F_{FB} and T_{Kola} were correlated with the NAO, unlagged and with time lags of 1 and 2 yr.

All further results presented relating to purely physical connections were based on direct, unlagged relations except when indicated by an av3 index. The F_{FB} series was closely linked to NAO_{av3} and GSNW (Fig. 3, all $P < 0.01$) and more weakly to PolEur ($r = 0.46$, $P < 0.05$; $r_s = 0.57$, $P < 0.01$). The T_{Kola} series showed a close fit to F_{FB} and NAO_{av3} (Fig. 3, all $P < 0.01$), whereas the links to PolEur ($r = 0.47$, $P < 0.05$; $r_s = 0.47$, $P < 0.05$) and GSNW ($r = 0.45$, $P < 0.05$; $r_s = 0.33$, $P < 0.10$) were less pronounced. The results were similar for the original, nondetrended, series.

Modeling F_{FB} by a pure first-order autoregressive model explained statistically ~30% of the total variability in the series. Additional autoregressive terms did not increase model performance. When NAO_{av3}, NAO, or GSNW was added to the first order autoregressive term, the model appropriate-

ness (as measured by AIC and SBC) and the level of explanation (as measured by R^2) increased profoundly. The best model included all the climate variables:

$$F_{FB} = 0.03a_1 + 0.23\text{NAO}_{av3} + 0.22\text{PolEur} + 0.14\text{GSNW}$$

($R^2 = 0.74$, AIC = 18.4, and SBC = 25.3, all but the a_1 term was significant at the 5% level). In Fig. 3, model estimates were compared with ''observed'' fluxes. A model that included NAO_{av3} and GSNW performed second best (as evaluated by AIC), $R^2 = 0.71$, AIC = 20.3, and SBC = 25.7, whereas the third-best model only included NAO_{av3} ($R^2 = 0.68$, AIC = 21.1, and SBC = 25.2). No lagged terms or averages of other explanatory variables than the NAO were statistically significant or improved the degree of model explanation.

A pure first-order autoregressive model for Barents Sea temperature, T_{Kola}, had R^2 of only 0.17 (AIC = 36.6 and SBC = 39.2). Adding autoregressive terms beyond the first order did not improve the degree of model explanation. The overall best fit was obtained for the model

$$T_{Kola} = 0.19a_1 + 0.15\text{NAO}_{av3} + 0.29\text{PolEur} + 0.13\text{GSNW}$$

($R^2 = 0.66$, AIC = 18.8, and SBC = 25.3; the NAO_{av3} and PolEur terms are significant at the 5% level and for GSNW $P = 0.06$). In Fig. 3, model estimates are compared with observed temperatures. It is perhaps surprising that the best model did not include F_{FB}, because this was found to be the single factor best that explained T_{Kola}. However, the second-best model, which included F_{FB}, PolEur, and GSNW ($R^2 = 0.65$, AIC = 19.4, and SBC = 25.9), and the third-best, which included all of NAO_{av3}, PolEur, and F_{FB} and GSNW ($R^2 = 0.67$, AIC = 19.5, and SBC = 27.3), only had a marginally poorer performance.

A pure first-order autoregressive model explained somewhat more than a third of the total variability in the abundance of cod at age 3, VPA_3. The best model (as evaluated by AIC) was

$$VPA_3 = 0.56a_1 + 0.07\text{NAO} + 0.34T_{Kola}$$

($R^2 = 0.56$, AIC = 33.86, and SBC = 38.89). Values estimated by this model are compared with actual VPA_3 values in Fig. 3. The second-best model included only NAO_{av3} ($R^2 = 0.53$, AIC = 33.95, and SBC = 37.72), and the third-best included NAO_{av3} and T_{Kola} ($R^2 = 0.55$, AIC = 34.31, and SBC = 39.34) (in addition to the first-order autoregressive term in both cases); these models performed only marginally poorer. Lagged terms did not improve the degree of explanation of the best models. However, note that all the models dealing with cod can be regarded as lagged, because we relate year-class strength at age 3 to climate conditions during the winter preceding spawning.

Discussion: Atlantic climate and Barents Sea oceanography—The statistically significant unlagged relationships documented in this paper demonstrate that much of the variability in the Barents Sea is affected by large-scale atmospheric forcing. On the basis of this, we feel that an expansion of the conceptual feedback model of Ådlandsvik and Loeng (1991) and Loeng et al. (1992) to include forcing external to the Barents Sea, is warranted. In addition, we suggest a mechanism through which climate may affect Barents Sea ecology (Fig. 4).

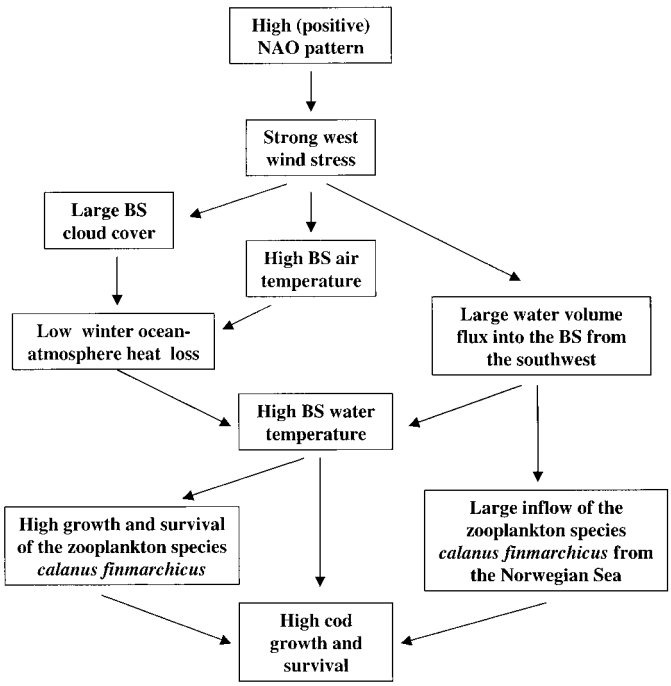

Fig. 4. Mechanisms suggested to link the NAO to variability in Barents Sea (BS) oceanography and ecology. A high (positive) NAO phase is connected to increased westerly winds over the North Atlantic. This effects BS water temperature through increasing both the volume flux of relative warm water from the southwest, cloud cover, and air temperature. Increased BS water temperature influences growth and survival of cod larvae both directly through increasing the development rate and indirectly through regulating the production of their main prey, nauplii of the copepod *Calanus finmarchicus.* Increased inflow from the zooplankton-rich Norwegian Sea further increases availability of food for the cod larvae. High food availability for larval and juvenile fish results in higher growth rates and greater survival through the vulnerable stages when year-class strength is determined (Ottersen and Loeng 2000).

The climatic system of the Barents Sea was studied by Ådlandsvik and Loeng (1991) who showed visually, for the period 1970–1986, that positive sea temperature anomalies, increased atmospherically driven inflow from the southwest, low air pressure, and decreased ice coverage occurred in synchrony and vice versa. The agreement in the fluctuations of all these variables led them to suggest that the climate of the Barents Sea oscillates between a warm and a cold state. A positive feedback mechanism is proposed where a warm period is characterized by low pressure, which leads to cyclonic circulation, increased inflow, less ice, larger heat flux, and lower pressure again. The opposite mechanism determines a cold period. These findings and the feedback hypothesis were later supported by Loeng et al. (1992). Although the visual impressions in these two papers seem convincing, statistical evidence for the relations was not given, partly because of lack of sufficiently long time series at the time. Furthermore, a connection between the NAO and Barents Sea climate was presented by Dickson et al. (2000) but again without any detailed statistical examination.

Loeng et al. (1992) pointed to three main factors that influence the temperature in the Kola section: (1) The volume flux of the inflowing Atlantic water, (2) the temperature of these water masses, and (3) the local heat flux to the atmosphere. They furthermore stated that the feedback model only considers the part of (1) that is caused by local wind forcing. In our opinion, this statement underestimates the importance of their own results. F_{FB} is directly related to wind strength and direction; positive F_{FB} values coincide with southwesterly, relatively mild winds. Thus, F_{FB} also provides information about (3) as an indicator of both air temperature and wind mixing.

Although external forcing factors, particularly the NAO, explains most of the variability in F_{FB} (Fig. 3), they do not explain much of the T_{Kola} variability beyond that covered by F_{FB}. We consider this an indicator of the NAO influencing Barents Sea temperature mainly through regulating local atmospheric conditions (barotropic part of [1] and [3] above) and to a lesser degree through influencing the inflowing water masses upstreams (baroclinic part of [1] and [2]).

Although models including several explanatory variables have an improved level of statistical explanation, our results also show that these climate variables are not statistically independent. Although GSNW separately explains as much of the variability in both F_{FB} and T_{Kola} as the NAO, GSNW performs poorly in models for T_{Kola}, including other explanatory variables. PolEur, on the other hand, seems to significantly improve models for T_{Kola}. This could be explained by both the NAO and GSNW being linked to Barents Sea temperature through the inflow from southwest, as estimated by F_{FB}, whereas PolEur more reflects the influence of processes over the Arctic Basin and thus captures a different part of the observed variability.

It is to be expected that variability in the GSNW is related to NAO variability, because the winds, and thus the NAO, are the driving forces of the subtropical gyre in the North Atlantic. We found a peak cross-correlation when GSNW lagged the NAO with 2 yr, which supports the results of Taylor and Stephens (1998). Although GSNW is correlated with F_{FB} and T_{Kola} and contributes to the models, this makes it difficult to accept GSNW as a driving force for Barents Sea climate. It is more likely that the correlations are due to all series being forced by the same large-scale atmospheric system (i.e., the westerlies and thus the NAO).

Cod and climate—Although several studies have presented evidence of high Barents Sea temperatures having a positive effect on cod recruitment in the region (see Ottersen and Sundby 1995 for references), a link between the NAO and Barents Sea cod recruitment has yet not been demonstrated. Here we have presented statistical results that indicate such a link and suggest a mechanism (Fig. 4) that links large-scale climate to cod recruitment through regional sea temperature and food availability. Earlier studies have shown favourable recruitment of cod to coincide with herring and haddock in the Barents Sea and hypothesized the cause to be large-scale temporal environmental variation having an influence common to the early stages of the species (Ottersen and Loeng 2000). Thus, the results presented here have implications for our understanding of recruitment variability not only of Barents Sea cod but also of herring and haddock.

Impact on marine ecology in the North Atlantic has previously been documented for both the NAO (Friedland et al. 1993; Fromentin and Planque 1996; Alheit and Hagen 1997) and GSNW (Taylor 1995). In this article, we have demonstrated that climatic processes on the scale of the North Atlantic basin may profoundly influence the ecology of the highly productive Barents Sea. These interrelations should improve our understanding of the ecosystem of the Barents Sea and may ultimately enhance our ability to manage the rich fish stocks of the area.

Geir Ottersen[1]

Institute of Marine Research
P.O. Box 1870, 1870 Nordnes
N-5024 Bergen, Norway

Nils Chr. Stenseth

Division of Zoology
Department of Biology
University of Oslo
P.O. Box 1050, Blindern
N-0316 Oslo, and
Institute of Marine Research
Flødevigen Marine Research Station
4817 His, Norway

References

ALHEIT, J., AND E. HAGEN. 1997. Long time climate forcing of European herring and sardine populations. Fish. Oceanogr. **6:** 130–139.

ÅDLANDSVIK, B., AND H. LOENG. 1991. A study of the climatic system in the Barents Sea. Polar Res. **10:** 45–49.

BLINDHEIM, J. 1989. Cascading of Barents Sea bottom water into the Norwegian Deep. Rapp. P.-V. Reun Cons. Int. Explor. Mer. **188:** 49–58.

BOCHKOV, Y. A. 1982. Water temperature in the 0–200m layer in the Kola-Meridian in the Barents Sea, 1900–1981. Sb. Nauchn. Tr. PINRO **46:** 113–122.

DICKEY, D. A., AND W. A. FULLER. 1979. Distribution of the estimators for autoregressive time series with a unit root. J. Am. Stat. Assoc. **74:** 427–431.

DICKSON, R. R. 1997. From the Labrador Sea to global change. Nature **386:** 649–650.

[1] Present address: Division of Zoology, Department of Biology, University of Oslo, P.O. Box 1050, Blindern, N-0316 Oslo, Norway (geir.ottersen@bio.uio.no).

Acknowledgements

This work was partly financed by the Research Council of Norway's project ''Variation in space and time of cod and other gadoids: the effects of climate and density dependence on population dynamics,'' project 134278/130. The work was done within the framework of the international Global Ocean Ecosystems Dynamics program. We thank Bjørn Ådlandsvik (IMR Bergen, Norway) for kindly providing the modeled flux values. We are also grateful to PINRO (Murmansk, Russia) for giving us temperature data from the Kola section. We further thank Karen Gjertsen (IMR) for preparing the map of Fig. 1. The comments and advice of three anonymous referees improved the paper greatly and are appreciated.

———, AND OTHERS. 2000. The Arctic Ocean response to the North Atlantic Oscillation. J. Climatol. **13:** 2671–2696.
FRIEDLAND, K. D., D. G. REDDIN, AND J. F. KOCIK. 1993. Marine survival of North American and European Atlantic salmon: Effects of growth and environment. ICES J. Mar. Sci. **50:** 481–492.
FROMENTIN, J.-M., AND B. PLANQUE. 1996. Calanus and environment in the eastern North Atlantic. II. Influence of the North Atlantic Oscillation on *C. finmarchicus* and *C. helgolandicus.* Mar. Ecol. Prog. Ser. **134:** 111–118.
HAENNINEN, J., I. VUORINEN, AND P. HJELT. 1999. Climatic factors in the Atlantic control the oceanographic and ecological changes in the Baltic Sea. Limnol. Oceanogr. **45:** 703–710.
HURRELL, J. W. 1995. Decadal trends in the North Atlantic Oscillation: Regional temperatures and precipitation. Science **169:** 676–679.
LOENG, H. 1991. Features of the physical oceanographic conditions of the Barents Sea. Polar Res. **10:** 5–18.
———, J. BLINDHEIM, B. ÅDLANDSVIK, AND G. OTTERSEN. 1992. Climatic variability in the Norwegian and Barents Seas. ICES Mar. Sci. Symp. **195:** 52–61.
———, V. OZHIGIN, AND B. ÅDLANDSVIK. 1997. Water fluxes through the Barents Sea. ICES J. Mar. Sci. **54:** 310–317.
OTTERSEN, G., B. ÅDLANDSVIK, AND H. LOENG. 2000. Predictability of Barents Sea temperature. Fish. Oceanogr. **9:** 121–135.
———, AND H. LOENG. 2000. Covariability in early growth and year-class strength of Barents Sea cod, haddock and herring: The environmental link. ICES J. Mar. Sci. **57:** 339–348.
———, AND S. SUNDBY. 1995. Effects of temperature, wind and spawning stock biomass on recruitment of Arcto-Norwegian cod. Fish. Oceanogr. **4:** 278–292.
PRIESTLEY, M. B. 1988. Non-linear and non-stationary time series analysis. Academic Press.
QUENOUILLE, M. H. 1952. Associated measurements. Butterworths.
SAKSHAUG, E. 1997. Biomass and productivity distributions and their variability in the Barents Sea. ICES J. Mar. Sci. **54:** 341–350.
SUNDBY, S., H. BJØRKE, A. V. SOLDAL, AND S. OLSEN. 1989. Mortality rates during the early life stages and year class strength of the Arcto-Norwegian cod (Gadus morhua L.). Rapp. P.-V. Reun Cons. Int. Explor. Mer **191:** 351–358.
SÆTERSDAL, G., AND H. LOENG. 1987. Ecological adaption of reproduction in Northeast Arctic Cod. Fish. Res. **5:** 253–270.
TAYLOR, A. H. 1995. North-South shifts of the Gulf Stream and their climatic connection with the abundance of zooplankton in the UK and its surrounding seas. ICES J. Mar. Sci. **52:** 711–721.
———, AND J. A. STEPHENS. 1998. The North Atlantic oscillation and the latitude of the Gulf Stream. Tellus **50A:** 134–142.
TERESHCHENKO, V. V. 1996. Seasonal and year-to-year variations of temperature and salinity along the Kola meridian transect. ICES CM **1996/C**:11, 24 p.
THOMPSON, K. R., AND F. H. PAGE. 1989. Detecting syncrony of recruitment using short, autocorrelated time series. Can. J. Fish. Aquat. Sci. **46:** 1831–1838.

Received: 2 August 2000
Amended: 22 June 2001
Accepted: 3 July 2001

Limnol. Oceanogr., 46(7), 2001, 1780–1783

Climatic warming causes regime shifts in lake food webs

Abstract—Spring clear water phases caused by grazing of zooplankton on algae are among the most spectacular and well-studied events in lake plankton dynamics. Such clear water phases are also important as windows of opportunity for recovery of aquatic vegetation and biodiversity in shallow waters. Here we use long time series from 71 shallow lakes to demonstrate that the probability of clear water phase increases with the temperature of lake water. We demonstrate that lake temperature has risen significantly over the past decades and is highly correlated with oscillations in the North Atlantic climate system. We also show a distinct climate-related shift in the timing of clear water phases in the shallow lakes as well as in an independent set of central European lakes. Simulations with a seasonally forced plankton model confirm that temperature rise is a plausible explanation for the observed changes.

A spring clear water phase is a common phenomenon in lakes (Sommer et al. 1986; Carpenter et al. 1993; Rudstam et al. 1993) but does not always occur. Indeed, most hypertrophic shallow lakes simply remain turbid throughout the year (Hosper and Meijer 1986; Sas 1989). Also, timing of the clear water phase can vary strongly (Scheffer et al. 1997). To check for relationships between occurrence of clear water phases and climatic conditions, we analyzed 257 seasonal patterns of chlorophyll *a* concentrations obtained between 1975 and 1991 from 71 shallow Dutch lakes sampled at least once every month. We selected the lowest summer chlorophyll *a* concentration between 1 April and 1 August in each annual time series and considered it a clear water phase if it represented a concentration of less than 5 μg L^{-1}. We related the occurrence of these clear water phases in Dutch lakes to a large scale climatic phenomenon known as the North Atlantic oscillation (NAO) using the NAO winter index (http://www.cgd.ucar.edu:80/cas/climind/). This climatic oscillation has been shown to influence a variety of ecosystems across the Northern Hemisphere (Ottersen et al. 2001) including several lakes (Weyhenmeyer et al. 1999; George 2000; Straile 2000; Straile and Adrian 2000). In addition to the NAO, we use the water temperature of one of our lakes (Lake Veluwe), where the temperature has been recorded on a daily basis since 1959 as a more direct indicator of changing climatic conditions for the Dutch lakes. To complement the analyses of the geographically and physically homogeneous set of Dutch lakes, we analyzed an independent data set of 136 seasonal time series of transparency from 28 central European lakes in which clear water phases were defined as the highest Secchi disk reading after the spring algal bloom.

The temperature of Lake Veluwe increased significantly since 1959 (Fig. 1). This trend occurs for water temperature in all seasons except spring (Table 1). Much of the variation in lake water temperature can be explained from the NAO winter